

SHEAR-INDUCED SEGREGATION OF FE-LIQUID IN PLANETESIMALS: COUPLING CORE FORMING COMPOSITIONS WITH TRANSPORT PHENOMENA . T. Rushmer¹, Nick Petford² and M. Humayun³

¹Department of Geology, University of Vermont, Burlington, VT 05405 (Tracy.Rushmer@uvm.edu) ²Center for Earth and Environmental Science Research, Kingston University, Kingston-Upon-Thames, UK ³National High Magnetic Field Laboratory & Department of Geological Sciences, Florida State University, Tallahassee, FL 32310.

Introduction: Timescales for first planetesimal accretion and differentiation have recently been under intense scrutiny. Although the isotopic data (mainly the decay of short-lived isotopes ^{182}Hf to ^{182}W) are still being gathered and interpreted, current data suggest that core formation in early planetesimals was likely a rapid process. The most recent estimations using high precision W isotopic data from iron meteorites [1,2] show a range in timing, but suggest some samples have formed in less than 2 Ma of solar system formation. Liquid iron-rich metal segregating from a molten silicate mantle (magma ocean) is a widely cited mechanism for segregating the Earth's core [3]. However, the short times for core formation based on W-Hf isotope systematics permit other segregation mechanisms for liquid metal to be active during core formation in growing planetesimals [4,5]. For example, deformation may assist the segregation of low degree metallic melts and may enhance both kinetics and efficiency of the physical segregation process. Here we report the results of a series of deformation experiments combined with modeling to investigate mechanisms of core-metal transport during planetesimal accretion and their associated liquid metal geochemical signatures. We then explore the relationship between melt fraction and porosity to compare the migration rate of liquid metal driven by buoyancy pressure gradients with a theoretical model of melt segregation in a deforming porous medium that takes into account the coupling between volume strain (dilatancy) and shear stress.

Geochemical Study and Results: Several key experiments performed on Kernouvé (H6), an ordinary chondrite (samples KM10, 11, 12, 17 and 24) show representative textures that develop during deformation as a function of liquid metal fraction and silicate melt percentage. Geochemical analyses on these samples have determined major element and siderophile concentrations in both Fe-S-Ni-O quench and Fe-Ni metal as a function of degree of melting. Data were collected using a JEOL 8900 Superprobe electron microscope and laser ablation ICP-MS.

LA-ICPMS analyses of individual large metal grains from Kernouvé starting material, quench Fe-S-Ni of different compositions and associated residual Fe-Ni metal from the deformation experiments were analyzed with a spot size varying between 25-50 μm [6].

The siderophile concentration data in Fe-S-Ni-O quench and associated Fe-Ni metal dynamically segregated at different degrees of partial melting were used to determine partition coefficients for different solid metal/liquid metal compositions as a function of degree of partial melting [6]. The geochemical results show the S content in the segregated Fe-rich liquid metal decreases with increasing degree of melting. The S content of the liquid metal affects the partitioning behavior of highly siderophile elements between solid (D_{sm}) and liquid metal (D_{lm}). An increase in porosity (liquid melt fraction) from c. 5 to 30% lowers $D_{\text{sm/lm}}$ for HSE by several orders of magnitude (Figure 1). The D values in the deformation experiments agree well with those determined from equilibrium experiments [7]. Textural analyses confirm the mobility of Fe-Ni-S-bearing liquids under conditions where the silicate matrix remains subsolidus or contains < 5% silicate liquid. At greater silicate melt fractions, metal-sulfide liquid geometry takes the form of immiscible, spherical shaped beads within the silicate melt. These gradually become coarser with increasing silicate melt fraction. Fe-Ni-S-O liquids occupy dilatant zones in regions where the olivine-pyroxene dominated silicate matrix has not undergone extensive melting or hydrofracture. Such textures are important in that they provide experimental evidence for the shear dilatant melt segregation model and confirms the presence of a dilatant deformational regime in the material prior to brittle failure.

Coupling geochemistry with metallic segregation rates and regimes: We apply a modeling approach that makes predictions on segregation rates of metallic liquid during porous flow and strain-induced migration and couples the results with metallic liquid geochemistry and highly siderophile element partitioning behavior.

The magnitude of the excess pore pressure,

defined as the difference between the fluid pressure minus the hydrostatic pressure, will drive melt segregation, or local flow rate. A model of melt segregation during matrix shear based on Biot's general theory of consolidation, modified to take into account the coupling between volume strain and shear stress has been recently developed and is relevant to the problem of liquid metal extraction [8]. The dilatant effect produced in the deformation experiments can be captured mathematically as a function of applied shear stress rate and can be solved analytically to yield explicit expressions for the excess pore fluid pressure, which is the local pressure gradient driving force for the liquid phase. This can be shown with Fe-liquid compositions as a function of melt fraction, at a given strain rate (Figure 1). Most importantly, the local Fe-rich liquid metal flow rate can also be calculated (Figure 2).

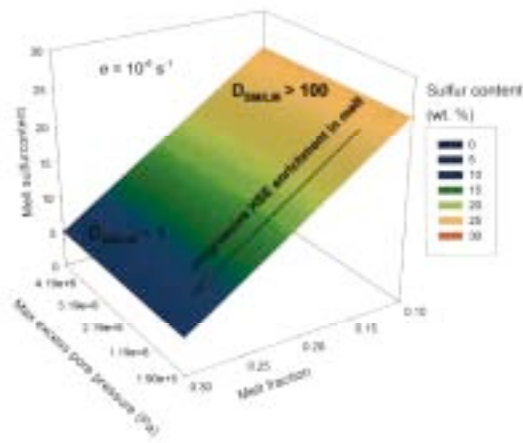


Figure 1: Relationship between Fe-liquid melt fraction, the associated sulfur content (S wt.%) and the calculated range in maximum excess melt (pore fluid) pressure at a fixed strain rate of 10^{-6} s^{-1} . Highest S contents (30 wt.%) correlate with lowest porosities. As solid metal residues are sensitive to changes in composition in Fe-Ni-S metallic liquids, the coupled variation between sulfur content and melt fraction will strongly influence the partitioning behavior (D) of the highly siderophile elements, which become preferentially concentrated in the liquid metal (LM) relative to the solid metal phase (SM) with decreasing melt S content [6.7].

The model is expressed in terms of shear strain rates, thus the fluid flow velocity is independent of intensive melt properties. Estimates of the flow rate resulting from shearing are calculated for strain rates ($\dot{\epsilon}$) in the interval 10^{-10} s^{-1}

to 10^{-5} s^{-1} , chosen to overlap with the experimental range, but also extended to faster rates of $> 10^{-3} \text{ s}^{-1}$, typical of high velocity impact loading. Figure 2 shows a summary of the shear-induced segregation regimes where the predicted flow velocities are plotted as a function of strain rate.

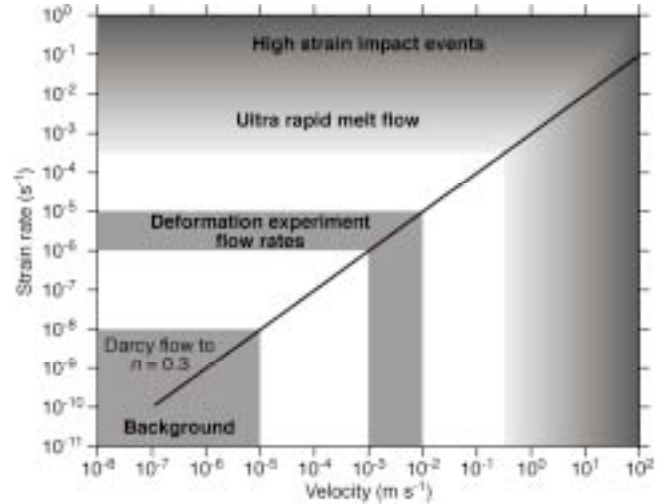


Figure 2: Calculated Fe metal liquid flow velocities versus strain rate ($\dot{\epsilon}$) in a deforming porous media. Estimates of flow based on Darcy's law for porosities up to 0.3 are shown for comparison (boxed region) and define a maximum velocity of 10^{-5} m s^{-1} corresponding to deformation-enhanced melt flow velocities at strain rates $< 10^{-8} \text{ s}^{-1}$. Hypervelocity impacts induce loading rates of $c. 10^{-1} - 10^0$, with predicted melt flow velocities $> 1 \text{ m s}^{-1}$.

Predicted characteristic timescales of Fe-liquid metal transport due to buoyancy effects (diapirism and porous flow) for a 100 km-sized planetesimal are $< 10^4$ years. During the latter (impact) stage of accretion that is likely to favor shear-enhanced melt flow, it is feasible that existing core material may be transported locally upwards back into the proto silicate mantle.

References:

- [1] Murkowski, A., et al. (2004) *EOS Fall AGU P31C-03*; [2] Kleine T., et al. (2004) *EOS Fall AGU P31C-04*; [3] Stevenson, D. (1990), in *The Origin of the Earth*, pgs. 231-249. [4] Walter, M.J., & Tronnes, R.J., (2004) *EPSL* 225, 253-269. [5] Yoshino, T. et al., (2004) *EPSL* 225, 253-269. [6] Rushmer, T., et al. (2004) *LPSC #1850* [7] Chabot, N., et al. (2003) *MAPS*, 38, 181-196. [8] Koenders, M. A. & Petford, N. (2000) *Geophys. Res. Lett.*, 27, 1231-1234.